Deception in taxonomy – the example of *Truncatellina rothi* (Hesse, 1916) (Pupilloidea: Truncatellinidae)

Jeannette Kneubühler
Natural History Museum Bern, Bernastrasse 15, 3005 Bern, Switzerland;
Institute of Ecology and Evolution, University of Bern, Baltzerstrasse 6, 3012 Bern, Switzerland;
jeannette.kneubuehler@nmbe.ch [corresponding author]

Hannes Baur
Natural History Museum Bern, Bernastrasse 15, 3005 Bern, Switzerland
Institute of Ecology and Evolution, University of Bern, Baltzerstrasse 6, 3012 Bern, Switzerland;

Eike Neubert
Natural History Museum Bern, Bernastrasse 15, 3005 Bern, Switzerland;
Institute of Ecology and Evolution, University of Bern, Baltzerstrasse 6, 3012 Bern, Switzerland

Kneubühler, J., Baur, H. & Neubert, E., 2020. Deception in taxonomy – the example of *Truncatellina rothi* (Hesse, 1916) (Pupilloidea: Truncatellinidae). – Basteria 84 (4-6): 146-154. Leiden. *Published 10 December 2020.*

In this study, *Truncatellina cylindrica* (A. Férussac, 1807), *Truncatellina rothi* (Hesse, 1916), and *Truncatellina haasi* Venmans, 1957 were investigated, and a lectotype for *Isthmia rothi* was selected. So far, the three species have only been defined by their shell morphology. Intensified collection efforts throughout the past 100 years increased the number of specimens available, and it has become increasingly questionable whether these three species represent different taxa. In this study 1070 specimens were photographed, and measurements of several shell traits were taken. A multivariate ratio analysis revealed that the morphological trait variation of *T. rothi* (and probably *T. haasi* as well) is mainly covered by the variability of *T. cylindrica*. There is no morphological evidence that the investigated specimens represent different taxa. A genetic study is needed to reveal possible cryptic clades.

Key words: Dwarf snails, Greece, morphometrics, shape pca, taxonomic revision, *Truncatellina*, Turkey.

INTRODUCTION

The shell of a land snail protects it from enemies or from drought and is influenced by environmental conditions as well as by the genetics that determine the bauplan. As a consequence, many land snails have similar shells. This similarity often makes it difficult to distinguish species or even genera. Adult land snails often develop a strong lip when they stop growing, and this distinguishes adults from juveniles (Goodfriend, 1986). In general, only adult specimens should be used for species identification. Nonetheless, serious difficulties for a reliable determination may remain. Differentiation criteria are often presented too optimistically (or uncritically) and cannot be applied correctly in practice.

In this study we test specimens collected by Peter Subai, who used the traditional shell-morphological approach to reliably distinguish the toothless species *Truncatellina cylindrica* (A. Férussac, 1807), *T. rothi* (Hesse, 1916) and *T. haasi* Venmans, 1957, whether the traditional criteria lead to an unambiguous determination of the species, or not.

Truncatellina rothi is described from the vicinity of Athens, and since then, it is recorded in large numbers from Greece, Cyprus (Vardinoyannis et al., 2012), and the western part of Turkey. Reinhardt (1916: 164), distinguished the new species from *T. cylindrica* by the following shell character states: 1) a "blunt" shell, 2) the peculiar shell form, where the upper whorls are wider if compared to the lower, 3) six strongly convex whorls, 4) a deep suture and 5) the ribbing pattern, where rib interspaces are wider than rib thickness. Upon receipt of a specimen from the Sea of Galilee, which superficially matched his new species, Reinhardt stated that *T. rothi* is common in the Eastern Mediterranean region. However, this is erroneous and based on a misidentification with a species, which today is known as *T. haasi*, a species known from the Levante region and Turkey (Pavlíček et al., 2008; Heller, 2009; Neubert et al., 2015).

The authorship of *T. rothi* has so far been attributed to Reinhardt (1916). Much to our surprise we noticed that *T. rothi*

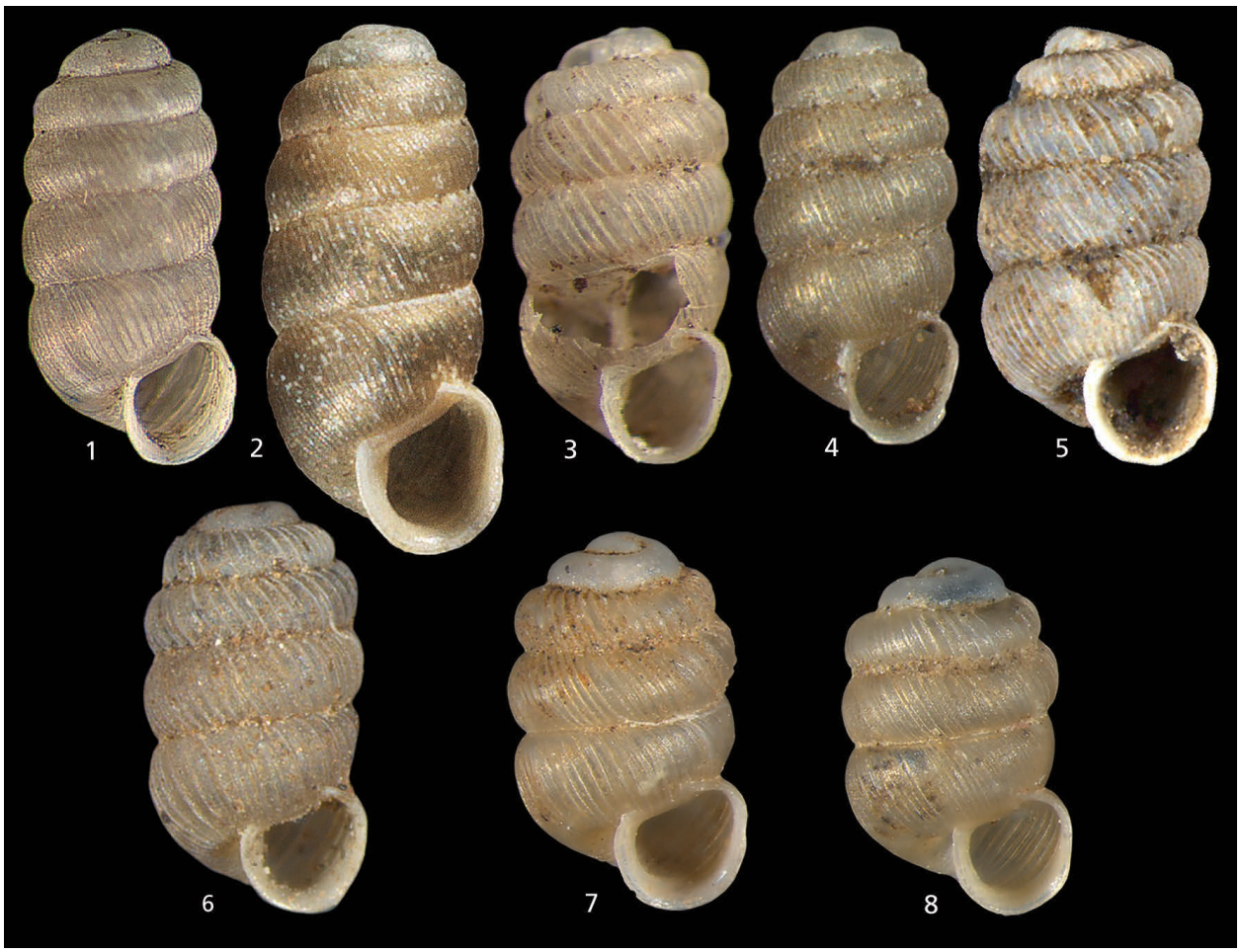

Figs 1-8. Species and specimens of *Truncatellina* as identified by authors. **1.** *T. cylindrica*, SMF 273803/3a, Istanbul, Büjük Ada, sh = 1.8 mm. **2.** Syntype *Pupa minutissima* var. *obscura*, ZMZ 514580, Greece, Janina, sh = 2.2 mm. **3.** Lectotype *Isthmia rothi*, SMF 4082, Greece, Athens, sh = 1.8 mm. **4.** *T. cylindrica*, NMBE 543359, Romania, Dambovicioara, Arges, sh = 1.79 mm. **5.** *T. cylindrica*, NMBE 543395, Greece, Kefalari Mountain, Korinthia, sh = 1.83 mm. **6.** *T. rothi*, NMBE 543991, Greece, Karpenissi, sh = 1.72 mm. **7.** *T. haasi*, NMBE 545643, Turkey, Silifke, cave Narlıkuyu Mağarisı, sh = 1.55 mm. **8.** *T. haasi*, NMBE 545642, Turkey, Side, Roman theatre, sh = 1.47 mm. All photographs × 25.

was already made available a few months earlier by Hesse in a paper on "Rumelia" in the same journal as Reinhardt (Hesse 1916: 121). It is based on the same specimens Reinhardt used for his description, and which once was collected by Roth. In parallel, Hesse included a specimen from Palestine (later described as *T. haasi*) from Tabgah, Lake Tiberias. We herewith select SMF 4082, "bei Athen", coll. Reinhardt ex Roth as lectotype for *Isthmia rothi* to fix the use of this name.

Due to intensified collection efforts in the past century, more specimens of the taxa *T. cylindrica, T. rothi* and *T. haasi* are now available for comparison (Figs 1-8). Recognising consistent differences between the three species became increasingly difficult the more specimens were inspected. Therefore, we hypothesise that the morphological trait variation of *T. rothi* and *T. haasi* is covered by the variability of *T. cylindrica*. This hypothesis is investigated by using morphometric methods. The specimens used in this study predominantly originate from the collection Subai, which is housed in the NMBE. Thus, they were identified by a single collector (except *T. haasi*, identified by Bank & Neubert), who utilized the aforementioned conchological traits to separate the species. Thus, any bias due to a probably differing view or concept could largely be excluded.

The distribution of *T. cylindrica*, *T. rothi*, and *T. haasi* is shown in Fig. 9. A distinct line of demarcation in the occurrence of *T. cylindrica* and *T. rothi* is observed in Greece with only one exception in Kefalari. In the south of Greece, all specimens were automatically identified as *T. rothi*. It is striking that in each locality, all specimens recorded were identified as either *T. cylindrica* or as *T. rothi*. Syntopy of different species is indirectly reported by Holyoak et al. (2012) for other species of *Truncatellina*. Thus, the "allopatric" situation for these two taxa in Greece is quite remarkable and probably caused by a "human" bias.

Fig. 9. Distribution of investigated *T. cylindrica* (violet dots), *T. rothi* (green dots), and *T. haasi* (brown dots) populations in Greece and Turkey as present (with a few exceptions) in the collection of Peter Subai (now NMBE).

MATERIAL AND METHODS

Abbreviations used for collections

NMBE = Natural History Museum Bern, Switzerland; SMF = Research Institute Senckenberg, Frankfurt am Main, Germany; ZMZ = Zoological Museum Zürich, Switzerland

Specimens investigated

The specimens from the Subai collection were collected in Greece and Turkey between 1975 and 2008. The total sample size comprised 1070 specimens. To investigate the trait variation in a large population of *T. cylindrica*, 100 randomly selected specimens from a single population in Romania (out of > 900) were used. We investigated 26 lots with 430 specimens identified as *T. cylindrica* and 33 lots with 520 specimens identified as *T. rothi* from Greece and Turkey. When possible, 20 randomly chosen adult specimens from each lot were photographed and measured. In less specious lots, at least 10 individuals were processed, whereas in some smaller lots, all specimens were assessed. Additionally, 18 specimens of *T. haasi* from Turkey and the Levante were included in the study. The lectotype of *Isthmia rothi* and a syntype of *Pupa minutissima* var. *obscura* Mousson, 1859 (ZMZ 514580, Janina, coll. Mousson ex Schläfli) were included. A detailed list of all the lots and their localities is presented in Table 1. The map in Figure 9 was produced with QGIS (2016, v2.18.12) using the Natural Earth data set.

Measurements

Each specimen was placed on a piece of clay in standardized vertical orientation with the aperture to the right and imaged with a Leica DFC425 microscope camera. Using an image processing program (IMS Client V15Q4, Imagic, Switzerland), the shell width (sw) and shell height (sh), the aperture width (aw) and aperture height (ah), the maximum diagonal diameter of the penultimate whorl (dpw), whorl width of the third whorl (ww), and the suture of the third whorl (s) were measured. All measurements were taken in µm. Whorl number (n) was counted from the aperture towards the apex (Fig. 10). In order to compare different specimens, the number of ribs per 500 µm (R_{500}) on the penultimate teleoconch whorl was counted. Measurements were chosen according to Reinhardt's differences (1916: 164) between *T. rothi* and *T. cylindrica*. We measured shell witdh (sw) and whorl width of the third whorl (ww) to account for Reinhardt's criteria 1) and 2). The number of whorls (n)

Species	NMBE.no.	Country	Location	Latitude	Longitude	Altitude [m]
cylindrica	543359	Romania	Dambovicioara, gorge 200-300 m N / Arges	45.454	25.219	970
cylindrica	543386	Greece	Nikissiani, south edge	40.947	24.144	350
cylindrica	543387	Greece	Akrovouni, 17.8 km for Pangéo-summit	40.915	24.147	1280
cylindrica	543320	Greece	Akrovouni, 11.6 km for Pangéo-summit	40.917	24.191	900
cylindrica	543424	Greece	Megali- and Mikra-Prespaseen, confluence	40.811	21.071	855
cylindrica	543417	Greece	Loutra Arides, entry to valley	40.972	21.912	450
cylindrica	543420	Greece	Prossotsani, 6 km N	41.223	23.969	340
cylindrica	543389	Greece	Kato Vrontou, 3.8 km, marble quarry	41.262	23.788	750
cylindrica	543451	Greece	Loutra Arides, entry to valley	40.972	21.912	450
cylindrica	543310	Greece	Stavroupoli, west edge next to river Nestos	41.203	24.706	120
cylindrica	543419	Greece	Aetia, 2.2 km E for Grevena, river breakthrough	40.074	21.202	1005
cylindrica	543302	Greece	Prossotsani, 6 km N	41.223	23.969	340
cylindrica	543395	Greece	Kefalari, 2 km E. mountain / Korinthia	37.915	22.532	730
cylindrica	543332	Greece	Gérmas, valley W	40.453	21.415	850
cylindrica	543383	Greece	Stavroupoli, west edge next to river Nestos	41.203	24.706	120
cylindrica	543468	Greece	Monastir Panagia Mavriotissa, 50-100 m W	40.505	21.279	640
cylindrica	543382	Greece	Zarkadia, 2.5 km NNE	41.029	24.642	450
cylindrica	543384	Greece	Profitis Ilias summit region / Ossa-mountains / Thessalia	39.795	22.671	1550
cylindrica	549113	Turkey	Bilecik, gorge underneath the mosque of Sey Edebali	40.144	29.99	400
cylindrica	549112	Turkey	Nusaybin, bridge over Çagcag Dere	37.09	41.215	470
cylindrica	549111	Turkey	right shore of Kizilirmak, 13 km SE Duragan / Sinop	41.340	35.140	180
cylindrica	549110	Turkey	Yeniçaga Gölü	40.782	32.034	988
cylindrica	543459	Turkey	Manavgat, bridge 13 km N of the cascade / Antalya	36.588	32.079	no data
cylindrica	547695	Turkey	Mekece	40.452	30.048	100
cylindrica	543390	Turkey	Road Akseki-Seydisehir, 1.5 km for Bozkir / Konya	37.220	31.936	1720
cylindrica	547694	Turkey	Gülümbe, 6 km before Bilecik	40.199	29.967	500
cylindrica	543558	Turkey	Dere (= Dereköy), west border / Bozkir / Konya	37.176	32.167	1260
rothi	544029	Greece	Klisura gorge, east edge, Ag. Eleusis / Etoloakarnania	38.501	21.376	350
rothi	543991	Greece	Karpenissi, 7.5 km WNW / Evritania	38.925	21.745	1250
rothi	544060	Greece	Klidonia, Turkish bridge, north end of the Vikos gorge / Ipiros	39.968	20.663	425
rothi	543999	Greece	Sandoméri, mountain Skollis / Ahaia	37.990	21.578	550
rothi	544073	Greece	Githio, 14 km for Areopoli / Lakonia	36.702	22.471	100
rothi	543995	Greece	Agios Pétros, 5.5 km SSE / Parnon mountains / Arkadia	37.311	22.578	970
rothi	544027	Greece	Agionori, 2 km for Limnes / Argolida	37.744	22.874	700
rothi	544078	Greece	Githio, 8.5 km for Areopoli / Lakonia	36.740	22.494	150
rothi	544072	Greece	Kalamata, 9.4 km, Artemissia gorge / Messinia	37.084	22.158	310
rothi	543993	Greece	Alivéri, west border / isle Évia	38.402	24.014	350
rothi	544041	Greece	Agios Ioannis, 1 km for Astros / Arkadia	37.354	22.640	750
rothi	544077	Greece	Astakos, mountain Veloutsa, SE-slope / Etoloakarnania	38.537	21.069	185
rothi	544037	Greece	Gliki, road to Koukoulii / Ipiros	39.332	20.603	160
rothi	543990	Greece	Paralia Sarandi, 3 km for Prodromos / Viotia	38.257	22.876	220
rothi	544020	Greece	Petralona, cave of Petralona / Makedonia	40.372	23.169	335
rothi	544031	Greece	Amfiklia, SE-border, small chapel, entry to the gorge / Fthiotida	38.631	22.596	500
rothi	544030	Greece	Gorge Klisura, W-edge, Ag. Eleusis / Etoloakarnania	38.501	21.368	290
rothi	544023	Greece	Argos, old castle, ruins / Argolida	37.639	22.715	250
rothi	544045	Greece	Kastritsa, mountain / Ipiros	39.639	20.915	500
rothi	544058	Greece	Langadia, 2 km for Arhea Olympia / Arkadia	37.682	22.015	850
rothi	544076	Greece	Petrona, W-edge / Etoloakarnania	38.926	21.407	500
rothi	544075	Greece	Triklino, 3.9 km for Alevrada / Etoloakarnania	38.954	21.466	no data
rothi	544004	Greece	Delfi, 2 km for Amfissa / Fokida	38.484	22.472	400
rothi	544070	Greece	Branch-off to Loutra Elefthero, 4.5 km W / Makedonia	40.721	24.060	30
rothi	544044	Greece	Vouliagméni, vis-à-vis of the isle Fléves / Atiki	37.809	23.784	20
rothi	544025	Greece	Theopetra, Kuvelci, 6 km SSE from Kalambaka / Thessalia	39.680	21.681	260
rothi	544063	Greece	Sarakina, 1 km W / Thessalia	39.661	21.628	180
rothi	544002	Turkey	Beskonak, bridge over Köprülü Canyon / Antalya	37.192	31.187	200
rothi	509508	Turkey	between Göynük and Çavusdere, 5 km W Çavusdere / Bolu	40.523	31.099	670
rothi	544003	Turkey	Kuru Cay, ca. 1 km E + 200 m N of the road / Konya	37.208	32.065	1420
rothi	544046	Turkey	Yarpuz, 14 km for Seydisehir / Konya	37.229	31.916	1610
rothi	544001	Turkey	Camlik (= Dalayman), 2 km SW. cave Maslialti-ini / Konya	37.344	31.622	1395
rothi	544000	Turkey	Road Beysehir-Akseki, 9 km for Yesildag / Konya	37.557	31.518	1200
haasi	549116	Turkey	Çesme, 10 rkm S Mordogan / Izmir	38.456	26.550	50
haasi	549115	Turkey	Anamur to Silifke, 4.6 km E Aydincik	36.152	33.372	40
haasi	549114	Turkey	Uzuncaburç 12 km SW	36.584	33.952	1070
haasi	548745	Turkey	Ruins of Ephesus	37.941	27.342	10
haasi	545643	Turkey	Narlikuyu Magarisi, 20 km NE Silifke / Silifke	36.449	34.102	140
haasi	545642	Turkey	Side, Ruins	36.768	31.391	10
haasi	517756	Jordan	Zobya	32.433	35.767	900
haasi	508204	Israel	limestone rock, upper Galil / Nahf	32.935	35.935	no data
haasi	508203	Jordan	Cave / Wadi Shwaib	31.970	35.723	no data

Table 1. Museum number, country of origin and geographical data of the records of *T. cylindrica, T. rothi* and *T. haasi* used for the study.

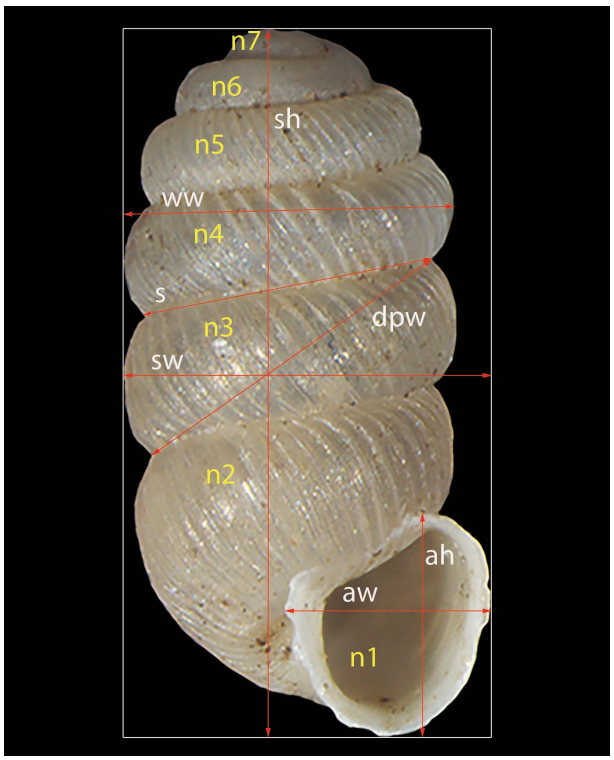

Fig. 10. Explanation of specimen measurements: shell height (sh), shell width (sw), aperture height (ah), aperture width (aw), maximum diagonal diameter of the penultimate whorl (dpw), whorl width of the third whorl (ww), and the suture of the third whorl (s). Whorl number (n) was counted from the aperture towards the apex.

were counted to meet Reinhardt's criteria 3). Criteria 4) is considered by the measurements of whorl width of the third whorl (ww) and suture of the third whorl (s) and criteria 5) is investigated by comparing the number of ribs per 500 µm (R_{500}).

Data analysis

A multivariate ratio analysis (MRA) was performed for shape analysis (R Development Core Team, 2016, v3.2.4). A slightly modified script from Baur & Leuenberger (2011, 2020) was used for the shape Principal Component Analysis (PCA) and the isosize calculation. Methods like PCA treat specimens as belonging to a single group, that is, specimens are not assigned to a particular group a priori. A PCA simply explores the most important pattern of variation in the entire dataset. Only later, when the data points are plotted on the first few axes, they are labelled by at least one factor variable, such as species or locality. But these have no influence on how principal components are calculated. In taxonomy, it is assumed that a PCA reveals the most interesting pattern of variation with respect to species separation. For instance, in sibling species, character variation related to species membership is usually expected to be more significant than variation related to any intraspecific population. Hence, it is reasonable to assume that PCA do detect species differences (Baur & Leuenberger, 2011, László et al., 2013, Baur et al., 2014).

To calculate the reliability, 30 randomly picked specimens, each 15 specimens of *T. cylindrica* and 15 specimens of *T. rothi,* were photographed and measured three more times in a random order. MANOVA was calculated in R using the comment manova(). A pairwise Wilcoxon test was performed in R to calculate rib numbers in *T. cylindrica, T. rothi,* and *T. haasi*. The lm() function in R was used for investigating any effect of the geographic variables on shape.

RESULTS

Shape and size analysis

Data reliability turned out to be very high (data not shown). Thus, measurement error is low and differences among groups should be traceable.

In order to identify traits which differentiate *T. rothi, T. cylindrica*, and *T. haasi*, a shape PCA was performed to explore the variation in shape of these three taxa. The shape PCA used the values of shell height (sh), shell width (sw), aperture height (ah), aperture width (aw), whorl width of the third whorl (ww), suture of the third whorl (s) and maximum diagonal diameter of the penultimate whorl (dpw) for each specimen. Only shape PC1 showed some differences in mean shape of forms, while in shape PC2 they are completely overlapping (data not shown). Hence, we continue only with shape PC1 and discard the remaining axes of the shape PCA. Shape PC1 differences are also highly significant as revealed by MANOVA ($p < 0.001$) (data not shown).

In Figure 11, isosize is plotted against shape PC1 to reveal a possible effect of allometry. This could be ruled out, as the three forms were not at all separated in isosize. Hence, size is no longer considered in the analysis.

The PCA ratio spectrum of shape PC1 (Fig. 12) showed that the differences among mean shape of the three forms was related to their main shell proportions (height to width). The variable shell height (shell.h) is at the upper end of the spectrum, while the five variables related with width, i.e. suture of the third whorl (suture.w), aperture width (aperture.w), shell width (shell.w), maximum diagonal diameter of the penultimate whorl (dp.w), and whorl width of the third whorl (whorl.w) are altogether at the lower end of the spectrum. The variable aperture height (aperture.h) lays in the middle of the spectrum and has thus no effect on shape PC1. One could thus say that generally the shape varied from the rather elongate shape of some *T. cylindrica* (and *T. rothi*) to the sturdier shape of some *T. haasi* (Fig. 11).

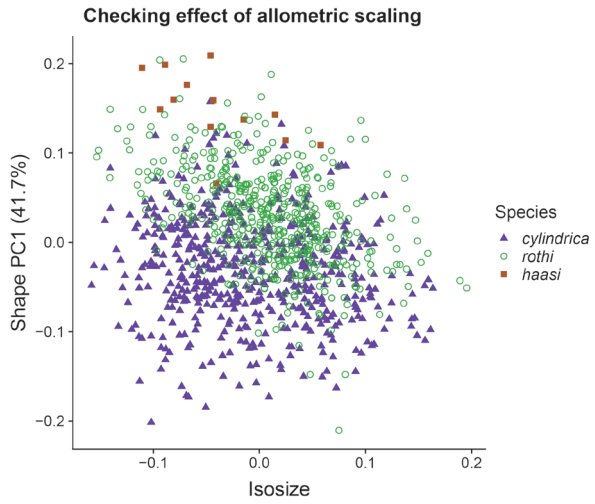

Fig. 11. Isosize plotted against shape PC1. Violet rectangles represent *T. cylindrica*, green circles represent *T. rothi*, and brown squares represent *T. haasi*.

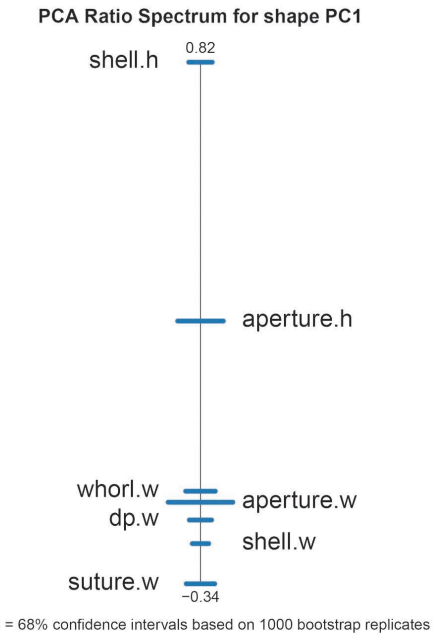

Fig. 12. The PCA ratio spectrum of shape PC1 with the shell measurements of shell height (shell.h), shell width (shell.w), aperture height (aperture.h), aperture width (aperture.w), maximum diagonal diameter of the penultimate whorl (dp.w), whorl width of the third whorl (whorl.w), and the suture of the third whorl (suture.w).

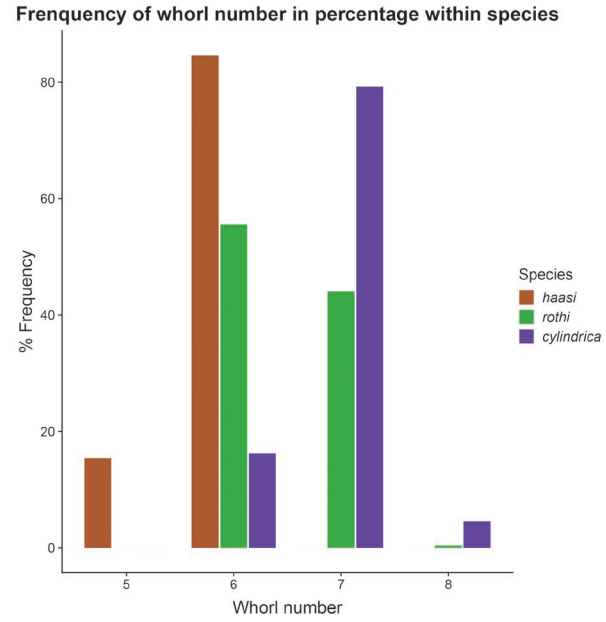

Fig. 13. Frequency of whorl number in percentage within the three species *T. cylindrica* (violet), *T. rothi* (green), and *T. haasi* (brown).

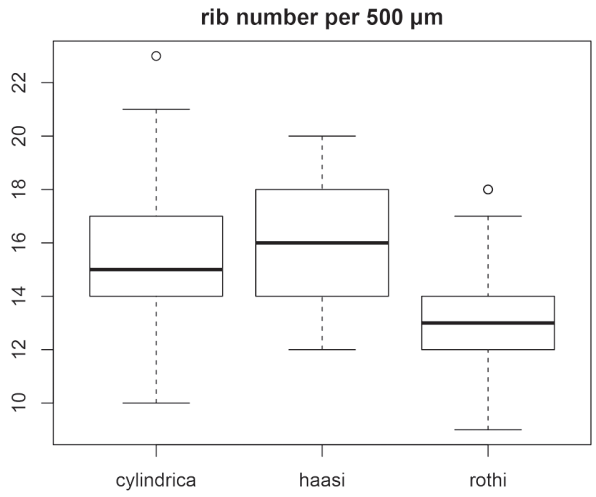

Fig. 14. Number of ribs per 500 µm of *T. cylindrica*, *T. rothi*, and *T. haasi*. A pairwise Wilcoxon test revealed a significant difference in the number of ribs per 500 µm ($p < 0.001$).

Meristic variables

All three forms show a variable number of whorls (Fig. 13), but are largely overlapping. Whorl number is clearly related to shell height, as the overall correlation between whorl number and shell height is highly significant (Spearman's rank correlation 0.541, $p < 0.001$).

As it is the case for the other characters, the number of ribs per 500 µm are almost completely overlapping in range (Fig. 14). Nevertheless, mean number is significantly smaller in *T. rothi* compared to the other forms (pairwise Wilcoxon test with Bonferroni correction p/3, $p < 0.001$).

	T. cylindrica	*T. haasi*	*T. rothi*	percentage correct
Truncatellina cylindrica	395	3	132	74.5
Truncatellina haasi	0	10	3	76.9
Truncatellina rothi	90	33	397	76.3

Table 2. LDA cross validation of the shell measurements of *T. cylindrica, T. rothi* and *T. haasi*.

LDA cross validation of shell measurements

The above analyses clearly show that it is impossible to separate any of the three "species" based on their shell morphology. There were some significant differences in mean shape, but as the ranges were largely overlapping, it was impossible to classify most specimens. For demonstrating, how difficult the separation was, we calculated LDA cross validation of the shell measurements. Although this time specimens are assigned to forms beforehand, the success of the classification was very low (Table 2). Only 76 % of *T. rothi*, 75 % of *T. cylindrica* and 77 % of *T. haasi* were correctly classified. Altogether these are very poor findings, as normally it should be possible that at least 95 % of specimens are classified correctly with LDA cross validation (Baur et al., 2014).

Modelling shape

We could show that the three forms cannot be separated using shell measurements and meristic data. However, the shape PCA clearly revealed that there is significant variation in shape PC1 (data not shown). We therefore applied a linear model to find out whether shape depended from geographic location or altitude. For some terrestrial snail species, a relation between altitude and shell traits has been suggested (e.g. Engelhard & Slik, 1994; Welter-Schultes, 2000). The model used in this study included latitude, longitude and altitude and allowed for their interaction. Only latitude was significant ($p < 0.01$) (Fig. 15).

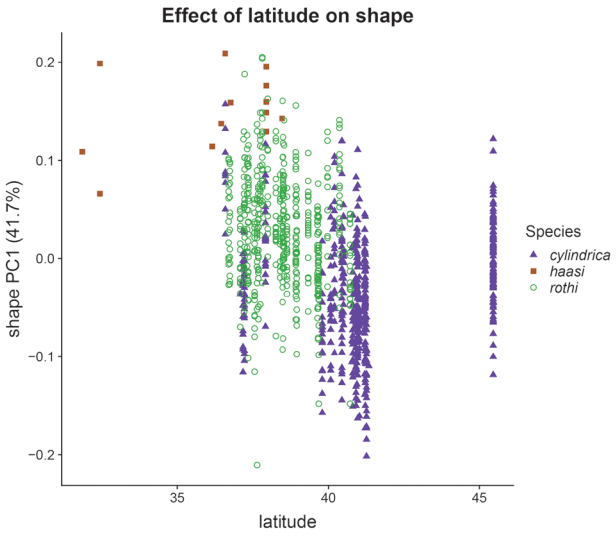

Fig. 15. Shape PC1 plotted against latitude for testing the effect of latitude on shape for *T. cylindrica* (violet rectangles), *T. rothi* (green circles), and *T. haasi* (brown squares).

DISCUSSION

The analysis of 1070 specimens shows that the variation of *T. rothi* is mainly covered by the variability of *T. cylindrica*. If a trait would have differentiated *T. rothi* from *T. cylindrica*, we would expect two distinct clusters of data points in the shape PCA with almost no overlap but a shift along shape PC1 or along shape PC2.

Figure 14 shows the distribution of the number of ribs per 500 µm. The reduction in number of ribs (Reinhardt, 1916: 164) was one important criterion for Reinhardt to separate the species *T. rothi* from *T. cylindrica*. Here it is shown that this difference exists in populations from Central to Southern Greece and Turkey. The difference between *T. cylindrica* and *T. rothi* is on average 1.8 ribs per 500 µm on the penultimate teleoconch whorl. However, Kemperman & Gittenberger (1988) showed that the ribbing pattern is influenced by humidity and temperature. Snails with many large ribs can retain more water between the shell surface and the substratum. This observation is supported by our data, and as ribbing pattern is obviously influenced by ecological factors, it cannot be considered as a reliable taxonomic trait discriminating between "species".

Figure 15 shows that the population from Romania covers almost the entire range of variation of the populations of Greece and Turkey. How then would it be possible to separate those three forms? Clearly this is not possible, and from a morphological species concept, the three forms have to be considered as belonging to one and the same, geographically slightly variable species. It should be stressed that it cannot be excluded that certain populations might be separable by means of genetic data. But, again, based on morphometric data of 1070 specimens over a wide distribution range, there is no justification for the recognition of three separate taxa from a morphological point of view.

In their paper in 2012, Holyoak et al. discuss the highly variable species *T. callicratis* (Scacchi, 1833), which can have

up to three denticles in the aperture, and thus can be easily distinguished from our species. However, there are many populations of this taxon known with a reduced apertural armature: toothless specimens (or even populations) are well known. This raises the question on how to distinguish such toothless *T. callicratis* specimens from the toothless *T. cylindrica*. After measuring numerous specimens of both taxa from France and mainly the Iberian Peninsula and Northern Africa, Holyoak et al. conclude in their key that both species are mainly distinguished by the "flatness" of their shells, which is quite a subjective trait. This assumption ignores morphological traits that remain to be explored in Central Europe, the Central Mediterranean area and Eastern Europe, where both taxa are known to occur. In Switzerland, both species are recorded from numerous localities, many of them in sympatry, and some probably even syntopic. The question remains whether both species (*T. cylindrica* and *T. callicratis*) represent biological entities, or whether traditional taxonomy is misguided by a single species, which is highly variable in its shell morphology, including all variations regarding the presence or absence of teeth (or lamellae as demonstrated by Nekola et al. (2018) for many species in the Vertiginidae).

CONCLUSION

After the analysis of 1070 specimens, no evidence was found for any significant shell-morphological differentiation as used by Hesse and Reinhardt (1916) between the three nominal taxa *T. rothi*, *T. cylindrica*, and *T. haasi*. The identification of shells as one of the three species seems to follow – especially with respect to *T. cylindrica* and *T. rothi* – an anthropocentric approach rather than a reflection of actually differing morphological traits. However, since the sample size of *T. haasi* is rather small and the distribution range of this species is not covered very well by our samples, we provisionally consider it as a distinct species until more specimens are investigated. But for *T. rothi* and *T. cylindrica* the classical shell-morphological approach is inappropriate and these two taxa should be synonymised. This does not necessarily mean that there are no other toothless *Truncatellina* species existing in Greece or Turkey. If so, a genetic study is needed to reveal such cryptic species, and this is also needed to clarify the taxonomic concept of *T. cylindrica* and *T. callicratis*.

ACKNOWLEDGEMENTS

We want to thank Thomas Inäbnit, Sarah Rohr, and Adrienne Jochum (all NMBE) for their valuable contribution to our study.

REFERENCES

Baur, H. & Leuenberger, C., 2011. Analysis of ratios in multivariate morphometry. —Systematic Biology 60: 813-825.

Baur, H., Kranz-Baltensperger, Y., Cruaud, A., Rasplus, J.Y., Timokhov, A.V. & Gokhman, V.E., 2014. Morphometric analysis and taxonomic revision of *Anisopteromalus* Ruschka (Hymenoptera: Chalcidoidea: Pteromalidae) – an integrative approach. — Systematic Entomology 39 (4): 691-709.

Baur, H. & Leuenberger, C, 2020. Multivariate Ratio Analysis (MRA): R-scripts and tutorials for calculating Shape PCA, Ratio Spectra and LDA Ratio Extractor (Version 1.02). Zenodo. http://doi.org/10.5281/zenodo.3892267.

Engelhard, G.H. & Slik, J.W.F., 1994. On altitude dependent characters in *Albinaria idaea* (L. Pfeiffer, 1849), with a revision of the species (Gastropoda Pulmonata: Clausiliidae). — Zoologische Mededelingen 68 (3): 21-38.

Férussac, J.B.L. d'Audebard de & Férussac, A.E.J. P.F. d'Audebard de, 1807. Essai d'une méthode conchyliologique Appliquée aux Mollusques fluviatiles et terrestres d'après la considération de l'animal et de son Test. Nouvelle édition augmentée d'une synonymie des espèces les plus remarquables, d'une table de concordance systématique de celles qui ont été décrites par Géoffroy, Poiret et Draparnaud, avec Müller et Linné, et terminée par un catalogue d'espèces observées en divers lieux de la France: xvi + 142 pp. Delance, Paris.

Goodfriend, G.A., 1986. Variation in land-snail shell form and size and its causes: A review. — Systematic Zoology 35 (2): 204-223.

Heller, J., 2009. Land snails of the land of Israel. Natural history and field guide: 1-360. Pensoft, Sofia/Moscow.

Hesse, P., 1916. Zur Kenntnis der Molluskenfauna von Ostrumelien. IV. Nachrichtsblatt der Deutschen Malakozoologischen Gesellschaft 48 (3): 113-122. Frankfurt am Main [14 July].

Holyoak, D.T., Holyoak, G.A. & Torres Alba, J.S., 2012. A reassessment of the species of *Truncatellina* (Gastropoda: Vertiginidae) in the Iberian Peninsula and Northwest Africa. — Iberus 30 (2): 7-33.

Kemperman, T.C.M. & Gittenberger, E., 1988. On morphology, function and taxonomic importance of the shell ribs in Clausiliidae (Mollusca: Gastropoda Pulmonata), with special reference to those in *Albinaria*. — Basteria 52 (1-3): 77-100.

László, Z., Baur, H., & Tóthmérész, B., 2013. Multivariate ratio analysis reveals *Trigonoderus pedicellaris* Thomson (Hymenoptera, Chalcidoidea, Pteromalidae) as a valid species. — Systematic Entomology 38 (4): 753-762.

Mousson, A., 1859. Coquilles terrestres et fluviatiles, recueillies dans l'Orient par M. le Dr. Alex. Schläfli. —

Vierteljahrsschrift der Naturforschenden Gesellschaft in Zürich, 4 (1): 12-36; 4 (3): 253-297.

Nekola, J.C., Chiba, S., Coles, B.F., Drost, C.A., Proschwitz, T. von, & Horsák, M., 2018. A phylogenetic overview of the genus *Vertigo* O.F. Müller, 1773 (Gastropoda: Pulmonata: Pupillidae: Vertigininae). — Malacologia 62 (1): 21-161.

Neubert, E., Amr, Z.S., Waitzbauer, W. & Al Talafha, H., 2015. Annotated checklist of the terrestrial gastropods of Jordan (Mollusca: Gastropoda). — Archiv für Molluskenkunde 144 (2): 169-238.

Pavlíček, T., Mienis, H.K., Raz, S., Hassid, V., Rubenyan, A. & Nevo, E., 2008. Gastropod biodiversity at the 'Evolution Canyon' microsite, lower Nahal Oren, Mount Carmel, Israel. — Biological Journal of the Linnean Society 93 (1): 147-155.

Reinhardt, O., 1916. Einige Bemerkungen über *Pupa minutissima* und Verwandte. — Nachrichtsblatt der Deutschen Malakozoologischen Gesellschaft 48 (4): 158-167. [1 October].

Scacchi, A., 1833. Osservazioni Zoologiche, 1: 1-12 [February]; 2: 13-27 [May]. Tipi della Società Tipografica, Napoli.

Vardinoyannis, K., Dimitropulos, S. & Mylonas, M., 2012. Atlandas ton salingarión tis Kíprou [Atlas of the snails of Cyprus]: 1-49. Cyprus Wildlife Society and Natural History Museum of Crete, Lefkosía [isbn 978-9963-8928-3-9].

Venmans, L.A.W.C., 1957. A new *Truncatellina* from Palestine. — Basteria 21 (1-2): 12-13.

Welter-Schultes, F.W., 2000. The pattern of geographical and altitudinal variation in the land snail *Albinaria idaea* from Crete (Gastropoda: Clausiliidae). — Biological Journal of the Linnean Society 71 (2): 237-250.

Internet sources

GenBank, National Center for Biotechnology Information, u.s. National Library of Medicine, 8600 Rockville Pike, usa; https://www.ncbi.nlm.nih.gov/genbank/ (last visit 06.iv.2020).

Imagic ims, ims Client v15q4, Imagic Bildverarbeitung ag, 8152 Glattbrugg, Switzerland, url http://www.imagic.ch/en/imagic-ims.

qgis (2016) v2.18.12; https://qgis.org/de/site/

R Development Core Team (2016) R: A language and environment for statistical computing. R Foundation for Statistical Computing, Vienna, Austria. isbn 3-900051-07-0, url http://www.R-project.org.